Insulin Receptor Internalization Defect in an Insulin-Resistant Mouse Melanoma Cell Line†

Matthew J. Androlewicz,‡ Dietrich F. Brandenburg,§ and Daniel S. Straus*,‡

Division of Biomedical Sciences and Department of Biology, University of California, Riverside, California 92521-0121, and Deutsches Wollforschungsinstitut, Aachen, West Germany D-51

Received February 24, 1989; Revised Manuscript Received July 27, 1989

ABSTRACT: Previous studies from this laboratory demonstrated that the PG19 mouse melanoma cell line does not exhibit a biological response to insulin, whereas melanoma x mouse embryo fibroblast hybrids do respond to insulin. To investigate the molecular basis of the insulin resistance of the PG19 melanoma cells, insulin receptors from the insulin-resistant melanoma cells and insulin-sensitive fibroblast x melanoma hybrid cells were analyzed by the technique of photoaffinity labeling using the photoprobe ^{125}I-NAPA-DP-insulin. Photolabeled insulin receptors from the two cell types have identical molecular weights as determined by SDS gel electrophoresis under reducing and nonreducing conditions, indicating that the receptors on the two cell lines are structurally similar. Insulin receptor internalization studies revealed that the hybrid cells internalize receptors to a high degree at 37 °C, whereas the melanoma cells internalize receptors to a very low degree or not at all. The correlation between ability to internalize insulin receptors and sensitivity to insulin action in this system suggests that uptake of the insulin–receptor complex may be required for insulin action in these cells. Insulin receptors from the two cell lines autophosphorylate in a similar insulin-dependent manner both in vitro and in intact cells, indicating that insulin receptors on the melanoma and hybrid cells have functional tyrosine protein kinase activity. Therefore, the block in insulin action in the PG19 melanoma cells appears to reside at a step beyond insulin-stimulated receptor autophosphorylation.

Insulin is an anabolic hormone that is an important regulator of metabolic homeostasis and growth (Goldfine, 1981; Straus, 1984). The first step in insulin action involves binding to a high-affinity receptor in the plasma membrane. This results in activation of a tyrosine protein kinase located in the cytoplasmic domain of the β-subunit of the receptor (Shia & Pilch, 1983), autophosphorylation of the β-subunit and subsequent further activation of the receptor kinase (Herrera & Rosen, 1986), phosphorylation on tyrosine residues of certain cellular proteins (Kadowaki et al., 1987; Bernier et al., 1987), and release from the plasma membrane of a soluble putative mediator of insulin action (Saltiel & Cuatrecasas, 1986). Beyond these early events, little is known about the intracellular molecular mechanisms by which insulin regulates metabolism and growth.

The binding of insulin to its receptor also results in endocytosis of the insulin–receptor complex. Two important consequences of endocytosis of insulin–receptor complexes are insulin degradation and removal of insulin receptors from the cell surface. An additional *functional* role, if any, of internalized insulin–receptor complexes has yet to be established. However, several lines of indirect evidence suggest that internalized insulin receptors may mediate some of the biological effects of insulin (Smith & Jarett, 1987; Podlecki et al., 1987).

To gain a further understanding of the mechanism of insulin action, we have undertaken a detailed examination of the PG19 mouse melanoma cell line, which is resistant to insulin, and a series of fibroblast x melanoma hybrids, which are responsive to insulin (Straus & Williamson, 1978; Coppock et al., 1980; Coppock & Straus, 1983; Kulkarni & Straus, 1983; Hecht & Straus, 1986). The PG19 melanoma cell lines does not respond to the growth-stimulatory effects of insulin, either under conditions of serum limitation or in hormone-supplemented serum-free medium. In contrast, hybrid cells constructed by crossing the melanoma cells with mouse fibroblasts respond to insulin under both conditions (Coppock et al., 1980; Coppock & Straus, 1983). Insulin also stimulates protein synthesis, inhibits protein degradation, and causes a rapid activation of a protein kinase enzyme that phosphorylates ribosomal protein S6 in the fibroblast x melanoma hybrids, but not in the parental melanoma cells (Coppock & Straus, 1983; Kulkarni & Straus, 1983; Hecht & Straus, 1986). These results suggest that the pathway of insulin action is blocked or uncoupled at an early step in the melanoma cells and that complementation for the insulin response occurs in the hybrids.

Previous equilibrium binding experiments indicated that the melanoma and hybrid cells had approximately equal numbers of insulin receptors, with similar binding affinities for insulin (Coppock et al., 1980). However, these studies did not rule out the possibility that insulin receptors on the melanoma cells might have a defect distal to hormone binding, such as defective signal transmission and/or tyrosine protein kinase activity. In the present study we used the photoaffinity probe ^{125}I-NAPA-DP-insulin[1] to examine the structure and endocytic processing of insulin receptors on the insulin-resistant melanoma cells and insulin-responsive hybrids. Although receptors

† This work was supported by NIH Grant DK21993.

* Address correspondence to this author at the Biomedical Sciences Division, University of California, Riverside, CA 92521-0121.

‡ University of California.

§ Deutsches Wollforschungsinstitut.

[1] Abbreviations: NAPA-DP-insulin, B2-[(2-nitro-4-azidophenyl)-acetyl]-des-Phe^{B1}-insulin; WGA, wheat germ agglutinin; FBS, fetal bovine serum; MEM, minimal essential medium; BSA, bovine serum albumin; NEM, *N*-ethylmaleimide; PMSF, phenylmethanesulfonyl fluoride; HEPES, *N*-(2-hydroxyethyl)piperazine-*N*′-2-ethanesulfonic acid; α-PY, anti-phosphotyrosine antibodies; IGF-I and -II, insulin-like growth factors I and II.

0006-2960/89/0428-9750$01.50/0

on both cell lines are structurally similar, receptors on the melanoma cells fail to undergo internalization to a significant degree, whereas receptors on the hybrid cells are internalized to a high degree. The correlation between ability to internalize insulin receptors and sensitivity to insulin action in this system suggests that uptake of the insulin–receptor complex may be required for insulin action.

Experimental Procedures

Materials. The following were purchased: $Na^{125}I$ from New England Nuclear, [γ-^{32}P]ATP (~3000 Ci/mmol) from Amersham, [^{32}P]orthophosphate (HCl free) from ICN, crystalline porcine insulin (25.7 units/mg) from Elanco, bovine trypsin, soybean trypsin inhibitor, *p*-nitrophenyl phosphate, and WGA–Sepharose from Sigma, WGA–agarose from Vector, IgGsorb from the Enzyme Center, Inc., Pansorbin from Calbiochem, Centricon 30 microconcentrators from Amicon, molecular weight standards from Bio-Rad and Sigma, and cell culture media from Gibco. B-10 anti-insulin receptor serum and anti-phosphotyrosine antibodies were generously provided by Dr. Phillip Gorden (National Institute of Diabetes, Digestive, and Kidney Diseases) and Dr. Morris White (Joslin Diabetes Center), respectively.

Cells and Cell Culture. The origin and growth properties of mouse melanoma cell line PG19 and the fibroblast x melanoma hybrid clone 100A have been described previously (Straus & Williamson, 1978; Coppock et al., 1980; Coppock & Straus, 1983; Kulkarni & Straus, 1983; Hecht & Straus, 1986). Cells were grown in minimal essential medium (MEM) containing 10% fetal bovine serum (FBS), penicillin (71 units/mL), and streptomycin (100 μg/mL) under an atmosphere of 95% air and 5% CO_2.

Iodination of NAPA-DP-insulin. The photoreactive insulin derivative B2-[(2-nitro-4-azidophenyl)acetyl]-des-Phe^{B1}-insulin was synthesized as described previously (Thamm et al., 1980). NAPA-DP-insulin was iodinated in the dark as previously described (Berhanu et al., 1982; Heidenreich et al., 1984).

Binding and Internalization of ^{125}I-NAPA-DP-insulin. Cells were plated at a density of 300 000 cells per 6-cm plate and allowed to grow in 3 mL of MEM/10% FBS at 37 °C for 2 days. The medium was then changed to MEM/0.3% FBS, and the plates were allowed to incubate overnight (18 h). The next day the confluent monolayers were washed once with MEM containing no serum and allowed to incubate 30 min at 37 °C in fresh serum-free MEM. The MEM was then aspirated, and 2 mL of cold binding buffer (20 mM HEPES, pH 7.6, 120 mM NaCl, 5 mM KCl, 1.2 mM $MgSO_4$, 10 mM glucose, 15 mM sodium acetate, 2 mM $CaCl_2$, 0.1% BSA) was added. Binding was initiated by adding 2×10^6 cpm/mL ^{125}I-NAPA-DP-insulin (25 ng/mL). Nonspecific binding was evaluated by adding 10 μg/mL unlabeled insulin to some dishes. Incubation was carried out in the dark at 4 °C for 2 h. The binding mix was then removed, and photolysis was carried out at 4 °C for 5 min by exposure to a long-wave (366-nm) UV lamp placed 10 cm from the cell monolayers. Each plate was then washed three times with 3 mL of cold PBS. To analyze labeled insulin receptors, cell monolayers were either solubilized immediately by addition of 800 μL of 1% NP-40 and 2 mg/mL bacitracin per plate, in the presence or absence of 1 mM *N*-ethylmaleimide (NEM), or trypsinized by addition of 2 mL of 400 μg/mL trypsin in PBS per plate. Plates containing trypsin were allowed to incubate for 15 min on ice. Trypsinization was stopped by the addition of 200 μL of soybean trypsin inhibitor (10 mg/mL in PBS). The mixture was then aspirated and the monolayer washed once with 3 mL of PBS. Trypsinized monolayers were then solubilized as above. Pooled trypsinized and nontrypsinized lysates were spun at 10000*g* for 1 min to clarify. The supernatants, containing soluble labeled receptors, were stored frozen at −20 °C. For insulin receptor internalization studies, photolyzed monolayers were further incubated for various times at 37 °C in 2 mL of serum-free F12/DME medium. At designated times the medium was aspirated, and the monolayers were washed once with 3 mL of cold PBS. Solubilization and trypsinization were performed as described above.

Gel Electrophoresis and Autoradiography. Samples of solubilized photolabeled insulin receptors were analyzed by SDS–polyacrylamide gel electrophoresis according to the method of Laemmli (1970). The samples were boiled for 5 min in sample buffer with the presence or absence of 50 mM dithiothreitol. Reduced samples were run on 7.5% resolving gels with 5% stacking gels. The bis(acrylamide):acrylamide ratio for both gels was 3:100. Nonreduced samples were run on 5–15% linear gradient gels with 3% stacking gels. The bis(acrylamide):acrylamide ratio in the resolving gel was 1:100 and in the stacking gel 3:100. The 1.5 mm thick gels were run at a consant current of 30 mA. Gels were stained, dried, and subjected to autoradiography at −70 °C by using Kodak X-Omat X-ray film and Du Pont Cronex intensifying screens.

Membrane Preparation and Protein Kinase Assays. Cells were plated at a density of 800 000 cells per 10-cm dish and allowed to grow to confluence. The cell monolayers were washed twice with PBS and harvested by scraping. The cell pellet was resuspended in hypotonic buffer (8.5 mM Tris-HCl, pH 7.8, 3 mM NaCl, 1 mM glucose, 0.2 mM $MgCl_2$, 0.1 mg/mL bovine serum albumin, 10 mM benzamidine hydrochloride, 2 mM PMSF) and allowed to swell for 15 min at 4 °C. The cells were then homogenized at 4 °C by using a Dounce homogenizer with loose-fitting piston. The homogenate was spun at 1000*g* for 10 min at 4 °C. The supernatant was then centrifuged at 50000*g* for 1 h at 4 °C. The high-speed pellet, containing crude plasma membranes, was stored at −70 °C.

For preparation of solubilized insulin receptors, the crude membrane pellet (from 20 10-cm dishes of cells) was dissolved in 1 mL of buffer containing 50 mM HEPES, pH 7.6, 1% Triton X-100, and 2 mM PMSF and homogenized by using a Dounce homogenizer. The homogenate was then centrifuged at 200000*g* for 30 min at 4 °C. An aliquot of the supernatant, which contained the solubilized receptor protein, was removed for protein assay (Wang & Smith, 1975). Aprotinin was then added to the remainder for a final concentration of 100 μg/mL. The crude receptor preparation was partially purified by using wheat germ agglutinin (WGA)–Sepharose chromatography. Solubilized receptor (5.1–6.4 mg total protein) was added to 0.3 mL of packed WGA–Sepharose at 4 °C, the flow-through material recycled three times, and the column washed with 50 mL of buffer (50 mM HEPES, pH 7.4, 0.1% Triton X-100). The bound insulin receptor was then eluted with the same buffer containing 200 mM *N*-acetylglucosamine. Fractions that contained the receptor (previously determined by using ^{125}I-labeled receptor on an identical column) were pooled and concentrated 5-fold by using Centricon 30 microconcentrators (final volume 800 μL). The concentrated eluates were used immediately.

Insulin-dependent phosphorylation of receptors was assayed essentially as described previously (Grigorescu et al., 1983). Briefly, 100-μL aliquots of WGA-purified receptors were first preincubated with various concentrations of insulin for 15 h at 4 °C. To initiate phosphorylation, each receptor aliquot was then added to a tube containing 50 mM HEPES, pH 7.6,

150 mM NaCl, 0.2% Triton X-100, 100 μCi of [γ-^{32}P]ATP, 10 μM unlabeled ATP, and 4 mM manganese acetate (total volume 400 μL). The reaction mixture was incubated for 10 min at 20 °C, and then terminated by the addition of 10x stop solution containing 500 mM NaF, 100 mM sodium pyrophosphate, 50 mM EDTA and 50 mM ATP. The phosphorylated insulin receptors were then immunoprecipitated by incubating with B-10 anti-receptor serum (Zick et al., 1983) at 1:50 dilution for 6 h at 4 °C. A final concentration of 5% IgGsorb was used to precipitate bound receptors. Final pellets were boiled for 5 min in Laemmli sample buffer containing 50 mM dithiothreitol. The proteins were analyzed by SDS gel electrophoresis using 7.5% resolving gels as described above. The gels were stained, dried, and subjected to autoradiography as described above. The incorporation of ^{32}P was quantified by scanning densitometry using an LKB Ultroscan XL laser densitometer.

Phosphorylation of the Insulin Receptor in Intact Cells. The procedures for labeling cell monolayers with [^{32}P]orthophosphate and immunoprecipitation of the phosphorylated insulin receptor have been described previously (Kulkarni & Straus, 1983; White et al., 1985, 1987). PG19 and 100A cells were plated at 2 × 10^6 cells per dish and allowed to grow to confluence in MEM containing 0.3% serum (3 days). The growth-arrested monolayers were washed three times with 5 mL of buffer containing 0.9% NaCl and 25 mM HEPES, pH 7.4. Phosphate-free MEM (3 mL) supplemented with 10 mM HEPES (pH 7.4) was then added to each dish, followed by [^{32}P]orthophosphate to a final concentration of 100 μCi/mL. The dishes were allowed to incubate at 37 °C for 2 h on a rocker platform (Bellco). Insulin was then added to the appropriate dishes to a final concentration of 1 μg/mL, and incubation was continued at 37 °C for an additional 5 min. The incubation was stopped quickly by aspirating the media and freezing the cell monolayers with liquid nitrogen. The cells were thawed and solubilized immediately at 4 °C with 2 mL of solution containing 50 mM HEPES, pH 7.4, 1% Triton X-100, 10 mM sodium pyrophosphate, 100 mM NaF, 4 mM EDTA, 2 mM sodium vanadate, 1 mg/mL aprotinin, and 2 mM PMSF per dish. The cell extracts were spun at 10000*g* in a microfuge for 10 min at 4 °C. Each supernatant, containing solubilized insulin receptors, was applied to a column containing 0.3 mL of packed WGA–agarose equilibrated with 50 mM HEPES, pH 7.4, 0.1% Triton X-100, 10 mM sodium pyrophosphate, 10 mM NaF, 4 mM EDTA, and 2 mM sodium vanadate. The flow-through material was recycled through the column twice, and the glycoproteins were eluted by the addition of buffer containing 300 mM *N*-acetylglucosamine. Ten fractions of 300 μL each were collected, and radioactivity in the fractions was measured by Cerenkov counting. The peak fractions were pooled and concentrated by using Centricon 30 microconcentrators. Phosphorylated insulin receptors were immunoprecipitated with anti-phosphotyrosine antibodies (α-PY) and Pansorbin as described previously (White et al., 1987). Phosphoproteins were eluted from precipitates with 10 mM *p*-nitrophenyl phosphate (PNPP) in 50 mM HEPES, pH 7.4, and 0.1% Triton X-100 overnight at 4 °C. Eluted proteins were analyzed by SDS–polyacrylamide gel electrophoresis under reducing conditions and subjected to autoradiography as described above.

Results

Comparison of Insulin Receptors on PG19 and 100A Cell Lines. Photolabeled insulin receptors from the melanoma cell line PG19 and the fibroblast x melanoma hybrid clone 100A were first analyzed by SDS gel electrophoresis under reducing conditions (Figure 1). The concentration of radiolabeled photoaffinity probe used in the labeling experiments was 25 ng/mL, which would be expected to predominantly label the insulin receptor rather than the IGF-I receptor. With both the PG19 and 100A cells, two bands (M_r 130 000 and 92 000) were observed (Figure 1). The labeling of these two bands was completely blocked by the addition of excess unlabeled insulin, indicating that the two bands represent subunits of the insulin receptor. The more intensely labeled M_r 130 000 band corresponds to the α-subunit of the insulin receptor. The more faintly labeled M_r 92 000 band most likely corresponds to the β-subunit of the receptor. A minor labeled band (M_r 66 000) was also seen under reducing and nonreducing conditions in some experiments. (This band was barely visible in the experiment shown in Figure 1 but was more visible in other experiments, such as those shown in Figures 2 and 3.) The labeling of the M_r 66 000 band was nonspecific, i.e., not competed for by excess unlabeled insulin. Therefore, this band does not represent a component of insulin receptor.

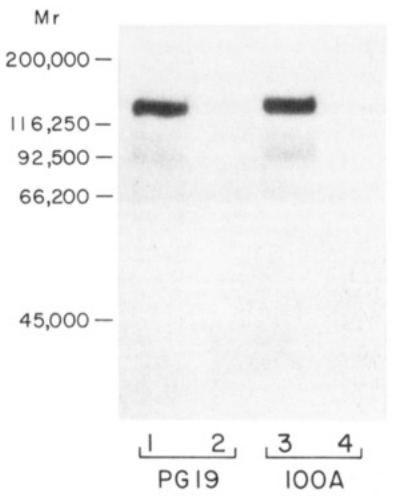

FIGURE 1: Identification of photolabeled insulin receptor subunits from PG19 melanoma cells and fibroblast x melanoma hybrid clone 100A cells under reducing conditions. Photoaffinity labeling, cell solubilization, and SDS–polyacrylamide gel electrophoresis were performed as described under Experimental Procedures. A 200-μL aliquot of cell extract from 1.5 × 10^6 total cells was run per lane of the reduced gel. The ^{125}I-NAPA-DP-insulin photolabel was allowed to bind to monolayers in the absence (lanes 1 and 3) or presence (lanes 2 and 4) of 10 μg/mL unlabeled insulin. PG19, lanes 1 and 2; 100A, lanes 3 and 4. Molecular weight markers: myosin (M_r 200 000), β-galactosidase (M_r 116 250), phosphorylase *b* (M_r 92 500), BSA (M_r 66 200), and ovalbumin (M_r 45 000).

Additional samples of photolabeled receptors solubilized in the presence or absence of *N*-ethylmaleimide (NEM) were run under nonreducing conditions (Figure 2). In the absence of NEM, several high molecular weight bands were specifically labeled for both PG19 and 100A (lanes 1 and 4). The molecular weights of the three highest bands were 430K, 380K, and 330K. In the presence of NEM, however, a much greater proportion of the label was found in the highest molecular weight 430K band, with a concurrent disappearance of the M_r 380K and 330K bands (lanes 2 and 5). The highest molecular weight species (430K) represents the $\alpha_2\beta_2$ tetrameric form of the receptor, while the 380K and 330K species correspond to partially reduced forms of the receptor which are generated during receptor extraction by an endogenous reducing agent (Helmerhorst et al., 1986). Inclusion of NEM in the extraction buffer blocks the appearance of the partially reduced forms of the receptor (Berhanu et al., 1982, 1983). The lower molecular weight bands on the gel, which were unaffected by

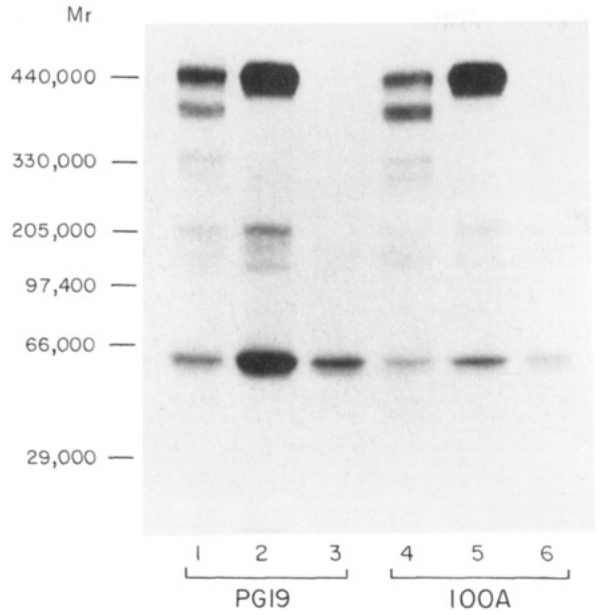

FIGURE 2: Identification of photolabeled insulin receptor subunits from PG19 and 100A cells under nonreducing conditions. A similar procedure to that described in Figure 1 was used. A 200-μL aliquot of cell extract from 1.5×10^6 total cells was run per lane of the nonreduced gel. The photolabel was allowed to bind to monolayers in the absence (lanes 1, 2, 4, and 5) or presence (lanes 3 and 6) of 10 μg/mL unlabeled insulin. Extraction of the nonreduced receptors was carried out in the absence (lanes 1, 3, 4, and 6) or presence (lanes 2 and 5) of 1 mM NEM: PG19, lanes 1–3; 100A, lanes 4–6. Molecular weight markers: fibronectin (M_r 440 000), thyroglobulin (M_r 330 000), myosin (M_r 205 000), phosphorylase *b* (M_r 97 400), BSA (M_r 66 000), and carbonic anhydrase (M_r 29 000).

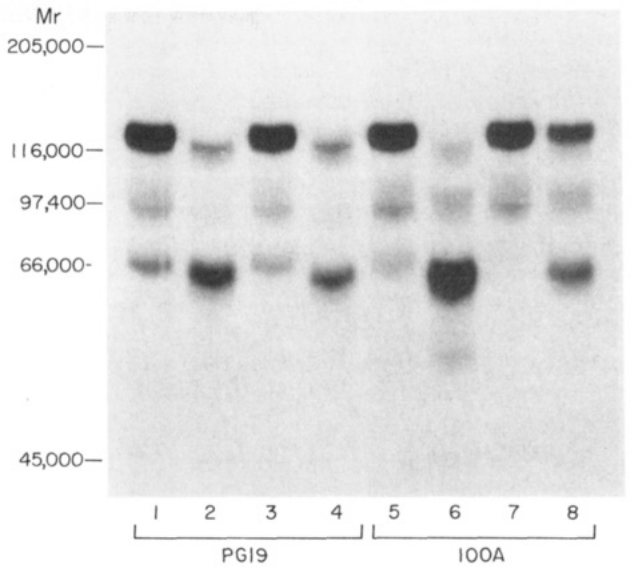

FIGURE 3: Insulin receptor internalization study. Amounts of extract run on the gel were the same as those run on the gels shown in Figures 1 and 2. Photolabeled monolayers were either solubilized (lanes 1 and 5); trypsinized and solubilized (lanes 2 and 6); incubated at 37 °C for 1 h and then solubilized (lanes 3 and 7); or incubated at 37 °C for 1 h and then trypsinized and solubilized (lanes 4 and 8). Samples were run on a 7.5% reducing gel. PG19, lanes 1–4; 100A, lanes 5–8. Molecular weight markers: myosin (M_r 205 000), β-galactosidase (M_r 116 000), phosphorylase *b* (M_r 97 400), BSA (M_r 66 000), and ovalbumin (M_r 45 000).

NEM, are most likely degradative fragments of the receptor. The observation that photolabeled receptors from the PG19 and 100A cells ran identically under both reducing and nonreducing conditions (Figures 1 and 2) suggests that they are structurally similar.

Insulin Receptor Internalization Studies. Although the insulin receptors on the insulin-resistant PG19 melanoma cells appeared to be structurally normal, the possibility remained that receptor internalization and processing by the PG19 cells may be abnormal. There is some indirect evidence that internalization of insulin receptors may be required to mediate certain biological effects of insulin (Smith & Jarett, 1987; Ueda et al., 1985). Therefore, internalization studies were performed to compare the fates of photolabeled insulin receptors on the PG19 and 100A cells. In these experiments, photolyzed monolayers were incubated at 37 °C to allow for uptake of the receptors via receptor-mediated endocytosis. In order to distinguish between internalized receptors and receptors that remained on the cell surface, an assay for sensitivity to trypsin was used (Berhanu et al., 1983).

A direct comparison of the fate of photolabeled receptors for the two cell lines is shown in Figure 3. Total cell-associated receptors after incubation with the photolabel at 4 °C (lanes 1 and 5), or identical samples treated with trypsin prior to solubilization (lanes 2 and 6), are shown. The trypsinization procedure effectively removed all the cell surface receptors as shown by lack of intact M_r 130 000 subunit. The tryptic fragments produced were of M_r 120 000, 60 000, and 50 000. Incubation of the photolabeled monolayers at 37 °C for 1 h followed by solubilization (lanes 3 and 7), or trypsinization prior to solubilization (lanes 4 and 8), revealed the occurrence of a trypsin-resistant band of M_r 130 000 for the 100A cells (lane 8), but not for the PG19 cells (lane 4). The results indicated that the 100A cells internalized receptors in a temperature-dependent manner, as shown by the existence of intact α-subunits after trypsin treatment. However, for PG19, no such intact α-subunits were detected after trypsin treatment, which indicated that receptors were not internalized in these cells.

Densitometric scanning of autoradiograms from three separate experiments revealed that ~30% of total labeled receptors became internalized after 1 h at 37 °C for the 100A cells. This degree of internalization is consistent with that found for insulin receptors on other cells, such as adipocytes (Berhanu et al., 1982). Quantitative analysis of the low degree of internalization for the PG19 cells was difficult due to interference of the M_r 120 000 tryptic fragment during the scanning procedure. Therefore, it could not be ruled out that a very small percentage of the receptors were internalized in the PG19 cells. Nevertheless, the results clearly indicate that 100A cells internalize insulin receptors to a much greater degree than PG19 cells.

To determine the kinetics of receptor uptake in the hybrid cells, a time course experiment was performed. The results shown in Figure 4, panel A, indicated that 100A cells exhibited a time-dependent increase in internalized receptors. Intact receptors could be detected after trypsin treatment as early as 10 min of incubation at 37 °C. Maximum levels of internalization were achieved by 30 min. In contrast, PG19 cells exhibited no such time-dependent increase in internalized receptors (Figure 4, panel B). These results further substantiate the lack of receptor uptake in the melanoma cells.

Autophosphorylation of Insulin Receptors in Vitro and in Vivo. There is an increasing amount of evidence that the insulin receptor tyrosine kinase is required to mediate certain biological responses to insulin, including the endocytosis of receptors (McClain et al., 1987; Hari & Roth, 1987; Chou et al., 1987). It was therefore of interest to examine the tyrosine kinase activities of the receptors from both the PG19 and 100A cell lines. In order to do this, insulin-dependent autophosphorylation of partially purified receptors was per-

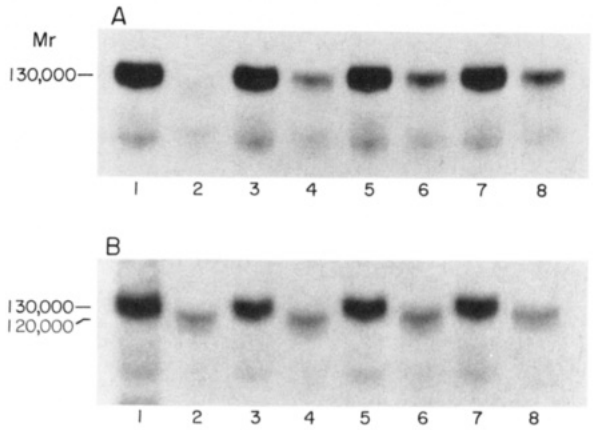

FIGURE 4: Internalization time courses. The procedure was similar to that described in Figure 3; however, incubation at 37 °C was carried out for various times. The times were 0 min (lanes 1 and 2), 10 min (lanes 3 and 4), 30 min (lanes 5 and 6), and 60 min (lanes 7 and 8). Odd lanes: monolayers were solubilized without trypsinization. Even lanes: monolayers were trypsinized and then solubilized. Panel A, 100A; panel B, PG19.

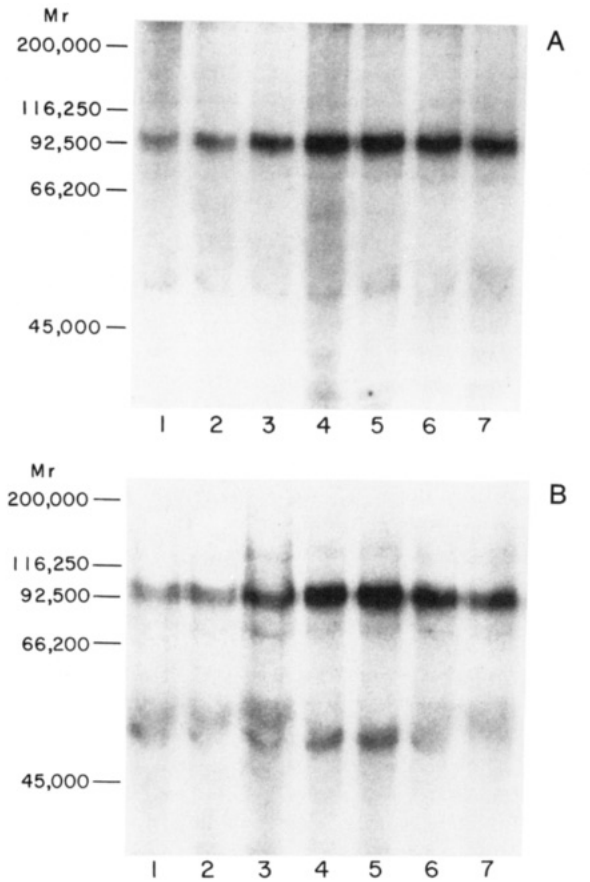

FIGURE 5: Autophosphorylation of insulin receptors from 100A and PG19 cells. Aliquots of partially purified insulin receptors (100 μL) were preincubated with varying amounts of insulin (0, 0.1, 1, 10, 100, 1000, and 10000 ng/mL; lanes 1–7) for 15 h at 4 °C. Receptor phosphorylation, immunoprecipitation, and gel analysis were performed as described under Experimental Procedures. Receptor protein was normalized for the two cell lines by applying the same amount of total protein to the WGA–Sepharose column (6.4 mg total soluble membrane protein). Panel A, 100A; panel B, PG19. Molecular weight markers: same as for Figure 1.

formed. Autoradiograms of gels showing insulin receptor autophosphorylation are shown in Figure 5. The results indicated that receptors from PG19 and 100A cells were autophosphorylated to a similar degree and in a similar insulin-dependent manner. In each case, a major band of M_r

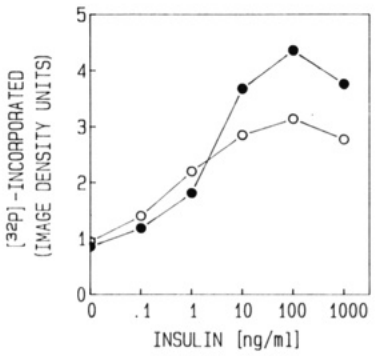

FIGURE 6: Quantitative analysis of autophosphorylation data. The autoradiograms shown in Figure 5 were scanned densitometrically, and incorporation of ^{32}P into the β-subunit of the receptor was quantified and expressed as image density units. (○) 100A; (●) PG19.

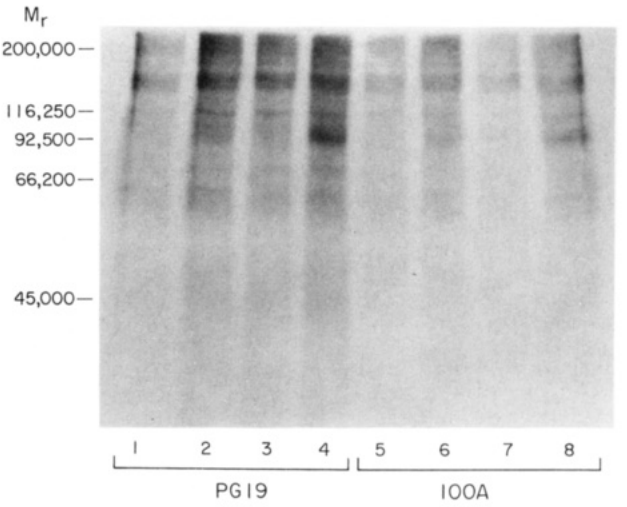

FIGURE 7: Phosphorylation of insulin receptors in intact cells. Confluent monolayers of growth-arrested PG19 and 100A cells in 10-cm dishes were labeled for 2 h with [^{32}P]orthophosphate and then incubated for 5 min in the presence (lanes 3, 4, 7, and 8) or absence (lanes 1, 2, 5, and 6) of insulin. Monolayers were solubilized as described under Experimental Procedures. Each lane represents an aliquot (200 μL) of WGA-purified cell extract immunoprecipitated in the presence (even lanes) or absence (odd lanes) of α-PY. Phosphoproteins were eluted from the precipitate with 10 mM *p*-nitrophenyl phosphate and analyzed on 7.5% reducing gels. Molecular weight markers: same as for Figure 1.

92000 was specifically phosphorylated in response to increasing amounts of insulin. This band corresponds to the β-subunit of the insulin receptor (Herrera & Rosen, 1986). Quantitative analysis of the data by scanning densitometry (Figure 6) revealed no significant difference in the degree of autophosphorylation between the melanoma and hybrid cells. In each case, maximum stimulation was achieved at an insulin concentration of 100 ng/mL with a half-maximal effect (ED_{50}) at approximately 1–3 ng/mL insulin. The activation of autophosphorylation at low concentrations of insulin strongly suggests that it is the insulin receptor and not the IGF-I receptor that is activated in these experiments.

To determine whether the insulin receptors autophosphorylated in vivo in response to insulin, PG19 and 100A cells were labeled with [^{32}P]orthophosphate at 37 °C and stimulated with insulin as described under Experimental Procedures. Labeled receptors were partially purified by affinity chromatography on WGA–agarose and immunoprecipitated with anti-phosphotyrosine antibodies (α-PY). The phosphoproteins detected in this manner for both cell lines are shown in Figure 7. A similar insulin-dependent increase in the phosphorylation of the M_r 92000 β-subunit of the insulin

receptor can be seen for both PG19 and 100A (lanes 4 and 8). Densitometric scanning of the autoradiogram revealed a 1.7-fold increase in the amount of ^{32}P incorporated into the M_r 92 000 band for both cell lines in the presence of insulin, compared with the minus insulin control (lane 4 compared with lane 2, and lane 8 compared with lane 6). The M_r 92 000 protein phosphorylated in response to insulin most likely represents the β-subunit of the insulin receptor. However, it is possible that the α-PY antibody may also have precipitated some IGF-I receptors, which have a β-subunit of similar size and which may have been activated by insulin at a concentration of 1 μg/mL. [We reported previously that the PG19 and 100A cells both had binding sites for MSA (rat IGF-II), although the exact number of type I and II IGF receptors on these cells has not been determined (Coppock et al.,1983).] Several other phosphoprotein bands of various molecular sizes appear on the film; however, these bands were not specifically immunoprecipitated with α-PY or affected by the presence of insulin.

Discussion

The use of the photoprobe ^{125}I-NAPA-DP-insulin allowed us to examine the structure and endocytic processing of the insulin receptors on the PG19 melanoma and the 100A fibroblast x melanoma hybrid cell lines. The results indicated that the receptors on the two cell lines are structurally similar, on the basis of the size of the photolabeled receptors under reducing and nonreducing conditions. Interestingly, the melanoma cells failed to internalize insulin receptors after incubation at 37 °C, whereas the hybrid cells did internalize receptors. This finding provides the first piece of evidence that a major functional difference exists between the insulin receptors on these two cell lines. Previous studies have shown that the 100A hybrid cells are responsive to various effects of insulin, including stimulation of DNA synthesis, stimulation of growth in serum-free medium, stimulation of protein synthesis, inhibition of protein degradation, and activation of a protein kinase enzyme that phosphorylates ribosomal protein S6 (Straus & Williamson, 1978; Coppock et al., 1980; Coppock & Straus, 1983; Kulkarni & Straus, 1983; Hecht & Straus, 1986). In contrast, the PG19 cells, which have approximately the same number of insulin binding sites, are not responsive to any of these effects of insulin.[2] Therefore, the finding that a functional difference exists between the receptors on these two cell lines provides some insight into the molecular basis for their dissimilar responses to insulin.

A number of studies have suggested a possible role for internalized insulin and/or insulin receptors in insulin action (Smith & Jarett, 1987; Podlecki et al., 1987; Ueda et al., 1985; Draznin & Trowbridge, 1982). Treatment of adipocytes with insulin plus monensin leads to a persistent partial activation of glucose transport and cAMP phosphodiesterase activity after removal of insulin from the medium (Ueda et al., 1985). This suggests that intracellular insulin–receptor complexes, which accumulate in the presence of monensin, retain residual capacity to stimulate glucose transport and phosphodiesterase activities. However, the residual activation is so weak that the same results can also be interpreted to indicate that the major signal for activation of glucose transport and phosphodiesterase activity is generated by the insulin–receptor complex prior to internalization. Other studies have demonstrated that some of insulin's actions, such as inhibition of protein degradation and stimulation of alanine transport, are blocked by inhibitors of insulin receptor uptake or insulin processing, suggesting a possible role for internalized insulin receptors and/or processed fragments of insulin in regulating these processes (Draznin & Trowbridge, 1982; Trowbridge & Draznin, 1986; Peavy et al., 1984). However, the inhibitors used in these studies may not be absolutely specific for hormone uptake and processing; thus, the results of the inhibitor experiments are equivocal. Finally, the recent observation that internalized insulin receptors are translocated to the nucleus has led to speculation that internalized receptors may have an effect on the long-term responses to insulin, such as the regulation of DNA and RNA synthesis (Smith & Jarett, 1987; Podlecki et al., 1987). However, there is at present no direct evidence supporting this hypothesis.

Our results provide new support to the notion that insulin receptor internalization plays a role in insulin action. As noted above, the 100A hybrid cells possess a number of well-documented responses to insulin. One early response to insulin that is exhibited by these cells is the rapid activation of a protein kinase enzyme that phosphorylates ribosomal protein S6 (Kulkarni & Straus, 1983; Hecht & Straus, 1986). It is interesting to note that the time course for this activation is similar to the time course for internalization of insulin receptors by the hybrid cells. This information, coupled with the knowledge that the melanoma cells exhibit no such activation of an S6 kinase (Kulkarni & Straus, 1983; Hecht & Straus, 1986), is consistent with the possibility that receptor internalization may play a role in mediating this response.

The observation that insulin receptors are not internalized, or are internalized to a very small degree in the PG19 cells, may provide at least a partial explanation as to why these cells are resistant to insulin. Lack of receptor internalization, although rare, has been reported for one other cell line, the IM-9 human lymphoblast cell line. Insulin receptors on IM-9 cells have been claimed to be internalized to a limited extent (Carpentier et al., 1978), not internalized at all (Berhanu et al., 1983), or shed from the cell surface and degraded (Berhanu & Olefsky, 1982). Furthermore, IM-9 cells are generally regarded as being biologically unresponsive to insulin (Kasuga et al., 1982). In a recent study of the regulation of IM-9 cell proliferation by hormones in serum-free media, we found that these cells may exhibit a very small growth response to insulin (Straus, 1988). However, this response represented only a 10% increase in growth over cultures incubated in the absence of insulin. Also, although the insulin effect was statistically significant in some experiments, it was not consistently observed in all experiments. These results are consistent with the idea that the IM-9 cells are at best marginally responsive to insulin.

The tyrosine kinase activity of the insulin receptor has recently been reported in several studies to be necessary for the proper transduction of the insulin signal (McClain et al., 1987; Hari & Roth, 1987; Chou et al., 1987; Russell et al., 1987; Ebina et al., 1987). These studies have shown that cells ex-

[2] We reported previously that insulin stimulated the uptake of [^3H]-2-aminoisobutyric acid ([^3H]AIB) in the PG19 cells (Coppock et al., 1980). This result contrasts with the insensitivity of the PG19 cells to all other biological actions of insulin tested to date. More recently, we reevaluated the amino acid uptake results using [^{14}C]-2-(methylamino)isobutyric acid ([^{14}C]MeAIB), which is more specific than AIB for the insulin-sensitive system A amino acid transport system (Kilberg et al., 1981; Shotwell et al., 1983). In seven independent experiments performed on different days, insulin stimulated MeAIB uptake by an average of 34% in the 100A hybrid cells. In contrast, insulin did not significantly stimulate MeAIB uptake in the PG19 melanoma cells. These results indicate that insulin does not stimulate system A amino acid transport in the melanoma cells, contrary to our previous conclusion (Coppock et al., 1980).

pressing insulin receptors that lack tyrosine kinase activity due to a mutation at the ATP-binding site fail to exhibit certain biological effects of insulin and also do not internalize insulin receptors. Interestingly, insulin receptors from both the PG19 and 100A cells appear to have functional tyrosine protein kinase activity, as shown by similar degrees of autophosphorylation both in vitro and in vivo. One could therefore conclude that factors other than tyrosine kinase activity are responsible for the lack of responsiveness to insulin and the lack of receptor internalization in the melanoma cells. It is possible that the melanoma cells lack the appropriate endogenous substrate for the insulin receptor and/or lack other signals that may be necessary for receptor internalization such as phosphorylation of the receptor by other serine/threonine-specific protein kinases (Hachiya et al., 1987).

Insulin resistance at the tissue level is important in the etiology of type II (non-insulin-dependent) diabetes mellitus, as well as a number of rare syndromes involving severe insulin resistance, including leprechaunism and type A syndrome of insulin resistance (Grigorescu et al., 1987; Yoshimasa et al., 1988; Kadowaki et al., 1988; Comi et al., 1987). There is currently a high level of interest in the molecular basis of insulin resistance in these diseases. In the case of type II diabetes, resistance to insulin appears to result from an impairment of the tyrosine protein kinase activity of the insulin receptor (Comi et al., 1987). In relation to the present study, it is of interest that insulin internalization into monocytes is also decreased in patients with type II diabetes mellitus (Trischitta et al., 1986). Since activation of tyrosine kinase activity of the receptor is linked to receptor-mediated endocytosis, the defect in insulin internalization in type II diabetes may be a secondary consequence of a defect in activation of the tyrosine kinase activity of the receptor. However, it is also possible that a low level of uptake of activated receptors may play a role in the insulin resistance of this disease.

ACKNOWLEDGMENTS

We thank Drs. Phillip Gorden and Morris White for their generous gifts of the anti-insulin receptor and anti-phosphotyrosine antibodies.

Registry No. Insulin, 9004-10-8; insulin receptor kinase, 88201-45-0.

REFERENCES

Berhanu, P., & Olefsky, J. M. (1982) *Diabetes 31*, 410–417.

Berhanu, P., Olefsky, J. M., Tsai, P., Thamm, P., Saunders, D., & Brandenburg, D. (1982) *Proc. Natl. Acad. Sci. U.S.A. 79*, 4069–4073.

Berhanu, P., Kolterman, O. G., Baron, A., Tsai, P., Olefsky, J. M., & Brandenburg, D. (1983) *J. Clin. Invest. 72*, 1958–1970.

Bernier, M., Laird, D. M., & Lane, M. D. (1987) *Proc. Natl. Acad. Sci. U.S.A. 84*, 1844–1848.

Carpentier, J.-L., Gorden, P., Amherdt, M., Van Obberghen, E., Kahn, C. R., & Orci, L. (1978) *J. Clin. Invest. 61*, 1057–1070.

Chou, C.-K., Dull, T. J., Russell, D. S., Gherzi, R., Lebwohl, D., Ullrich, A., & Rosen, O. M. (1987) *J. Biol. Chem. 262*, 1842–1847.

Comi, R. J., Grunberger, G., & Gorden, P. (1987) *J. Clin. Invest. 79*, 453–462.

Coppock, D. L., & Straus, D. S. (1983) *J. Cell. Physiol. 114*, 123–131.

Coppock, D. L., Covey, L. R., & Straus, D. S. (1980) *J. Cell. Physiol. 105*, 81–92.

Draznin, B., & Trowbridge, M. (1982) *J. Biol. Chem. 257*, 11988–11993.

Ebina, Y., Araki, E., Taira, M., Shimada, F., Mori, M., Craik, C. S., Siddle, K., Pierce, S. B., Roth, R. A., & Rutter, W. J. (1987) *Proc. Natl. Acad. Sci. U.S.A. 84*, 704–708.

Goldfine, I. D. (1981) in *Biochemical Actions of Hormones* (Litwack, G., Ed.) Vol. 8, pp 273–305, Academic Press, New York.

Grigorescu, F., White, M. F., & Kahn, C. R. (1983) *J. Biol. Chem. 258*, 13708–13716.

Grigorescu, F., Herzberg, V., King, G., Meistas, M., Elders, J., Frazer, T., & Kahn, C. R. (1987) *J. Clin. Endocrinol. Metab. 64*, 549–556.

Hachiya, H. L., Takayama, S., White, M. F., & King, G. L. (1987) *J. Biol. Chem. 262*, 6417–6424.

Hari, J., & Roth, R. A. (1987) *J. Biol. Chem. 262*, 15341–15344.

Hecht, L. B., & Straus, D. S. (1986) *Endocrinology 119*, 470–480.

Heidenreich, K. A., Brandenburg, D., Berhanu, P., & Olefsky, J. M. (1984) *J. Biol. Chem. 259*, 6511–6515.

Helmerhorst, E., Ng, D. S., Moule, M. L., & Yip, C. C. (1986) *Biochemistry 25*, 2060–2065.

Herrera, R., & Rosen, O. M. (1986) *J. Biol. Chem. 261*, 11980–11985.

Kadowaki, T., Koyasu, S., Nishida, E., Tobe, K., Izumi, T., Takaku, F., Sakai, H., Yahara, I., & Kasuga, M. (1987) *J. Biol. Chem. 262*, 7342–7350.

Kadowaki, T., Bevins, C. L., Cama, A., Ojamaa, K. Marcus-Samuels, B., Kadowaki, H., Beitz, L., McKeon, C., & Taylor, S. I. (1988) *Science 240*, 787–790.

Kasuga, M., Karlsson, F. A., & Kahn, C. R. (1982) *Science 215*, 185–187.

Kilberg, M. S., Handlogten, M. E., & Christensen, H. N. (1981) *J. Biol. Chem. 256*, 3304–3312.

Kulkarni, R. K., & Straus, D. S. (1983) *Biochim. Biophys. Acta 762*, 542–551.

Laemmli, U. K. (1970) *Nature 227*, 680–685.

McClain, D. A., Maegawa, H., Lee, J., Dull, T. J., Ullrich, A., & Olefsky, J. M. (1987) *J. Biol. Chem. 262*, 14663–14671.

Peavy, D. E., Edmondson, J. W., & Duckworth, W. C. (1984) *Endocrinology 114*, 753–760.

Podlecki, D. A., Smith, R. M., Kao, M., Tsai, P., Huecksteadt, T., Brandenburg, D., Lasher, R. S., Jarett, L., & Olefsky, J. M. (1987) *J. Biol. Chem. 262*, 3362–3368.

Russell, D. S., Gherzi, R., Johnson, E. L., Chou, C.-K., & Rosen, O. M. (1987) *J. Biol. Chem. 262*, 11833–11840.

Saltiel, A. R., & Cuatrecasas, P. (1986) *Proc. Natl. Acad. Sci. U.S.A. 83*, 5793–5797.

Shia, M. A., & Pilch, P. F. (1983) *Biochemistry 22*, 717–721.

Shotwell, M. A., Kilberg, M. S., & Oxender, D. L. (1983) *Biochim. Biophys. Acta 737*, 267–284.

Smith, R. M., & Jarett, L. (1987) *Proc. Natl. Acad. Sci. U.S.A. 84*, 459–463.

Straus, D. S. (1984) *Endocr. Rev. 5*, 356–369.

Straus, D. S. (1988) *Cell Tissue Kinet. 21*, 115–122.

Straus, D. S., & Williamson, R. A. (1978) *J. Cell. Physiol. 97*, 189–198.

Thamm, P., Saunders, D., & Brandenburg, D. (1980) in *Insulin: Chemistry, Structure and Function of Insulin and Related Hormones* (Brandenburg, D., & Wollmer, A., Eds.) pp 309–325, de Gruyter, Berlin.

Trischitta, V., Gullo, D., Squatrito, S., Pezzino, V., Goldfine, I. D., & Vigneri, R. (1986) *J. Clin. Endocrinol. Metab. 62*, 522–528.
Trowbridge, M., & Draznin, B. (1986) *Horm. Metab. Res. 18*, 156–158.
Ueda, M., Robinson, F. W., Smith, M. M., & Kono, T. (1985) *J. Biol. Chem. 260*, 3941–3946.
Wang, C.-S., & Smith, R. L. (1975) *Anal. Biochem. 63*, 414–417.
White, M. F., Takayama, S., & Kahn, C. R. (1985) *J. Biol. Chem. 260*, 9470–9478.
White, M. F., Stegmann, E. W., Dull, T. J., Ullrich, A., & Kahn, C. R. (1987) *J. Biol. Chem. 262*, 9769–9777.
Yoshimasa, Y., Seino, S., Whittaker, J., Kakehi, T., Kosaki, A., Kuzuya, H., Imura, H., Bell, G. I., & Steiner, D. F. (1988) *Science 240*, 784–787.
Zick, Y., Kasuga, M., Kahn, C. R., & Roth, J. (1983) *J. Biol. Chem. 258*, 75–80.

The DNase I Sensitive State of "Active" Globin Gene Chromatin Resists Trypsin Treatments Which Disrupt Chromatin Higher Order Structure†

Martha Lundell‡ and Harold G. Martinson*
Department of Chemistry and Biochemistry and Molecular Biology Institute, University of California, Los Angeles, California 90024

Received May 2, 1989; Revised Manuscript Received July 28, 1989

ABSTRACT: Active genes in higher eukaryotes reside in chromosomal domains which are more sensitive to digestion by DNase I than the surrounding inactive chromatin. Although it is widely assumed that some modification of higher order structure is important to the preferential DNase I sensitivity of active chromatin, this has so far not been tested. Here we show that the structural distinction between DNase I sensitive and resistant chromatin is remarkably stable to digestion by trypsin. Chick embryonic red blood cell nuclei were subjected to increasing levels of trypsin digestion and then assayed in the following three ways: (1) by gel electrophoresis for histone cleavage, (2) by sedimentation and nuclease digestion for loss of higher order structure, and (3) by dot-blot hybridization to globin and ovalbumin probes for disappearance of preferential DNase I sensitivity. We have found that chromatin higher order structure is lost concomitantly with the cleavage of histones H1, H5, and H3. In contrast, the preferential sensitivity of the globin domain to DNase I persists until much higher concentrations of trypsin, and indeed is not completely abolished even by the highest levels of trypsin we have used. We therefore conclude that the structural distinction of active chromatin, recognized by DNase I, does not reside at the level of higher order structure.

Active genes in higher eukaryotes reside in chromosomal domains which are more sensitive to digestion by DNase I than the surrounding inactive chromatin [Weintraub & Groudine, 1976; reviewed in Reeves (1984)]. This DNase I sensitive state generally encompasses both the active genes themselves and the nontranscribed regions of chromatin flanking them (Alevy et al., 1984; Jantzen et al., 1986; Lawson et al., 1982; Scott et al., 1987). This is in contrast to various transcriptionally induced perturbations of chromatin which have been characterized and which are limited both temporally and spatially to the regions actually undergoing transcription (Allegra et al., 1987; Chen & Allfrey, 1987; Cohen & Sheffery, 1985; Dorbic & Wittig, 1987; Johnson et al., 1987; Moreno et al., 1986; Smith et al., 1984; Wu & Simpson, 1985). The transcriptionally induced perturbations probably represent additional structural alterations beyond those which are responsible for the DNase I sensitivity of the large DNase I sensitive domains which almost always extend beyond the transcription units themselves.

Speculation regarding the structure of active chromatin has focused on three classes of chromatin component: the H1 histones (which includes H5), the core histone amino-terminal segments, and the two smaller high mobility group (HMG)[1] proteins. Both the H1 histones and the core histone amino-terminal segments have been implicated in the maintenance of higher order structure in chromatin [Allan et al., 1986; Böhm & Crane-Robinson, 1984; Hilliard et al., 1986; Klingholz & Strätling, 1982; Morse & Cantor, 1986; reviewed in Reeves (1984)], and elimination or modification of these components is generally presumed to relax higher order structure and facilitate chromatin activity (Nelson et al., 1986; Reeves, 1984; Ridsdale & Davie, 1987; Rocha et al., 1984; Weintraub, 1984). The two small HMG proteins have an unknown structural role but appear to be specific components of active chromatin (Dorbic & Wittig, 1987; Brotherton & Ginder, 1986; Reeves, 1984; Rocha et al., 1984).

Although it is clear that the H1 histones are important determinants of higher order structure, the vagaries of higher order structure itself leave the exact role played by H1 unclear (Felsenfeld & McGhee, 1986; Pederson et al., 1986). Three properties of chromatin are attributable to the H1 histones: the dinucleosomal periodicity of chromatin (Klingholz & Strätling, 1982; Thoma & Koller, 1981), the folding of the elementary nucleosomal filament into the 30-nm fiber [reviewed in Reeves (1984)], and aggregation (Jin & Cole, 1986). Active regions of chromatin are frequently proposed to be partially depleted in H1 (Reeves, 1984; Ridsdale & Davie, 1987; Rocha et al., 1984), to be associated with particular H1

† This work was supported by U.S. Public Health Service Grant GM35750.
* Author to whom correspondence should be addressed at the Department of Chemistry and Biochemistry, University of California.
‡ Present address: Department of Biological Chemistry and Molecular Pharmacology, Harvard Medical School, Boston, MA 02115.

[1] Abbreviation: HMG, high mobility group.

0006-2960/89/0428-9757$01.50/0